Technical Report, UMINF 15.06, Dept. of Computing Science, Umea University, 2015

Time-Domain Sensitivity Analysis for Conductivity Distribution in Maxwell's Equations

Emadeldeen Hassan, Eddie Wadbro, and Martin Berggren

Abstract

We present expressions for the derivatives of the outgoing signal in coaxial cables with respect to the conductivity distribution in a specific domain. The derived expressions can be used with gradient-based optimization methods to design metallic electromagnetic devices, such as antennas and waveguides. We use the adjoint-field method to derive the expressions and the derivation is based on the 3D time-domain Maxwell's equations. We present two derivative expressions; one expression is derived in the continuous case and the second is derived based on the FDTD discretization of Maxwell's equations, including the uniaxial perfectly match layer (UPML) to simulate the radiation boundary condition. The derivatives are validated through a numerical example, where derivatives computed by the adjoint-field method are compared against derivatives computed with finite differences. Up to 7 digits precision matching is obtained.

1. INTRODUCTION

Maxwell's equations predict the propagation and the interaction of electromagnetic waves in different media. The electromagnetic properties of a medium are usually described through the constitutive parameters; permeability, permittivity, and conductivity [1]. Generally, electromagnetic devices are designed based on the distribution of the constitutive parameters in a certain domain with a specific configuration. The goal of electromagnetic analysis is to compute the response of a device to a certain excitation source, whereas in electromagnetic design, we aim to find a suitable distribution of the constitutive parameters that achieves a required response [2].

One way to design electromagnetic devices with particular properties is to formulate the design problem as an optimization problem, where an objective function F is extremized over a set of design variables $\boldsymbol{p}$ that parametrizes one or more of the constitutive parameters inside a design domain. Generally, the optimization process starts with an initial distribution of the design variables and proceeds, through a number of iterations, aiming to successively improve the objective function F. When gradient-based optimization is used, the derivatives of the objective function with respect to the design variables (also known as the gradient vector) are crucial to find a suitable updates. The gradient of the objective function can be defined as

$$\frac{\partial F}{\partial \boldsymbol{p}} = \Big[\frac{\partial F}{\partial p_1}, \frac{\partial F}{\partial p_2}, \dots, \frac{\partial F}{\partial p_M}\Big]^T, \tag{1}$$

where M is the total number of design variables.

If there is an explicit relation between the design vector $\boldsymbol{p}$ and the objective function F, the gradient vector can be directly computed. However, typically in electromagnetic design problems, the objective function and the design variables are implicitly related through Maxwell's equations. In this case, the gradient vector might be computed either with finite difference approximations or by using adjoint-field methods.

Finite differences approximate the derivatives through formulas like

$$\frac{\partial F}{\partial p_i} \approx \frac{F(\boldsymbol{p} + s e_i) - F(\boldsymbol{p})}{s} \qquad i = 1, \dots, M, \tag{2}$$

where e_i is the i^{th} column of the identity matrix, and s is a small step length. We note that, $M + 1$ objective function evaluations are required to approximate the gradient vector by using expression (2), which indicates

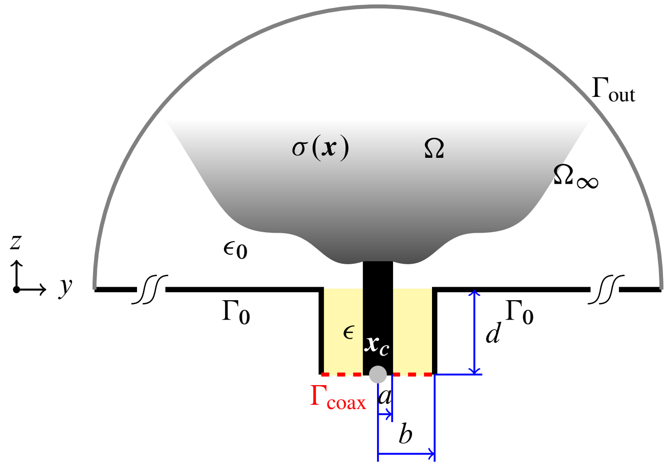

Figure 1. An illustration of the physical problem: the analysis domain Ω_∞ is bounded by the boundaries Γ_{out}, Γ_0, and Γ_{coax}, respectively. Included in Ω_∞ is a subdomain Ω, where a conductivity distribution $\sigma(\boldsymbol{x})$ can be located.

that finite differences are computationally expensive when a large number of design variables is used. Moreover, the accuracy obtained by using expression (2) might be poor and results in slow convergence of optimization problems.

On the other hand, the adjoint-field methods evaluate the gradient vector in an efficient and accurate way [2–9]. For each objective function, typically adjoint-field methods compute the exact gradient for an arbitrary number of design variables by using only two solutions to the system governing equations. Computing the derivatives with the adjoint-field methods is thus efficient when the number of design variables is much larger than the number of objective functions. The main difficulties with the adjoint-field methods are the derivation and the numerical computation of the derivative expression. Moreover, a separate sensitivity analysis is required for each objective function.

Two approaches might be used to obtain derivative expressions with the adjoint-field methods; a continuous approach and a discrete approach. In the continuous approach, the derivative expression together with an adjoint system are derived in the continuous case, then both are discretized for the numerical calculations. Although the continuous approach describes the computations in a clear way, typically numerical discretization of the obtained expressions makes the accuracy of the computed gradient grid-dependent. In the discrete approach, first the system of equations is discretized, then the derivative expression and the adjoint system are derived based on the discretized system. By using the discrete approach to compute the gradient vector, exact accuracy up to roundoff can be achieved.

In this work, we formulate a problem based on the 3D Maxwell's equations, where a coaxial cable is connected to a design domain Ω that holds a conductivity distribution $\sigma(\boldsymbol{x})$. The analysis domain is excited with an electromagnetic signal that might be introduced to the analysis domain either through the coaxial cable or from any other source. By using the adjoint-field method, we derive expressions to the derivative of the outgoing signal in the coaxial cable with respect to the conductivity distribution $\sigma(\boldsymbol{x})$. Two derivative expressions are introduced; one derived based on the continuous formulation and another expression derived based on the FDTD discretization of the problem. Finally, we give a numerical example to validate the derivatives computations. We compare derivatives calculated by using the adjoint-field method with derivatives calculated by using the finite differences, where we use the Richardson extrapolation [10] to improve the accuracy of the derivatives obtained by finite differences.

2. PHYSICAL PROBLEM AND GOVERNING EQUATIONS

We consider the problem setup shown in Figure 1. An analysis domain Ω_∞ holds a subdomain Ω, where a conductivity distribution $\sigma(\boldsymbol{x})$ is located, with $\boldsymbol{x}$ representing a point inside Ω. The analysis domain Ω_∞ is connected, through a ground plane Γ_0 located at $z = 0$, to a coaxial cable that has a center core and a metallic shield with radii a and b, respectively. We denote by Γ_{coax} the annular surface generated by a cross section at $z = -d$ through the dielectric part of the coaxial cable. The boundary $\partial\Omega_\infty$ consists of three parts: Γ_{coax}, where the incoming (outgoing) signal through the coaxial cable can be specified (recorded), Γ_{out} where an incoming (outgoing) far-field signals can be specified (recorded), and the perfect electric conductor, which comprises the ground plane Γ_0, the metallic shield, and the surface of the center core of the coaxial cable for $-d < z \le 0$.

We consider the initial-boundary-value problem

$$
\begin{aligned}
&\frac{\partial}{\partial t}\mu \boldsymbol{H} + \nabla \times \boldsymbol{E} = \boldsymbol{0} && \text{in } \Omega_\infty, \text{ for } t > 0, && \text{(3a)}\\
&\frac{\partial}{\partial t}\epsilon \boldsymbol{E} + \sigma \boldsymbol{E} - \nabla \times \boldsymbol{H} = \boldsymbol{0} && \text{in } \Omega_\infty, \text{ for } t > 0, && \text{(3b)}\\
&\boldsymbol{n} \times \boldsymbol{E} = \boldsymbol{0} && \text{on } \Gamma_0, \text{ for } t > 0, && \text{(3c)}\\
&\boldsymbol{E}_t = \frac{V}{\log b/a}\frac{\boldsymbol{x} - \boldsymbol{x}_{\text{c}}}{|\boldsymbol{x} - \boldsymbol{x}_{\text{c}}|^2} && \boldsymbol{x} \in \Gamma_{\text{coax}}, \text{ for } t > 0, && \text{(3d)}\\
&I = \int_{C_r} \boldsymbol{H} \cdot d\boldsymbol{l} && C_r \subset \Gamma_{\text{coax}}, \text{ for } t > 0, && \text{(3e)}\\
&\boldsymbol{E}_t + Z_0\, \boldsymbol{n} \times \boldsymbol{H} = \boldsymbol{W}^- && \text{on } \Gamma_{\text{out}}, \text{ for } t > 0, && \text{(3f)}\\
&V + Z_{\text{c}} I = g(t) && \text{on } \Gamma_{\text{coax}}, \text{ for } t > 0, && \text{(3g)}\\
&\boldsymbol{E}|_{t=0} = \boldsymbol{0}, && && \text{(3h)}\\
&\boldsymbol{H}|_{t=0} = \boldsymbol{0}, && && \text{(3i)}
\end{aligned}
$$

where μ, ϵ, and σ are the permeability, the permittivity, and the conductivity of the medium, respectively; $\boldsymbol{E}_t = \boldsymbol{E} - \boldsymbol{n}(\boldsymbol{E} \cdot \boldsymbol{n})$ with $\boldsymbol{n}$ defined as the outward unit normal vector; C_r specifies a circle belongs to Γ_{coax} and with radius $a < r < b$; $Z_0 = \sqrt{\mu_0/\epsilon_0}$ is the free space intrinsic impedance where μ_0 and ϵ_0 are the free space permeability and the permittivity, respectively.

Equation (3a) and equation (3b) are the Maxwell's equations that govern the relation between the electric field $\boldsymbol{E}$ and the magnetic field $\boldsymbol{H}$ in the upper half space $z > 0$. Equation (3c) is the boundary condition for a perfect electric conductor. The right-hand side of expression (3d) is the formula for the electric field in any transversal cross section in an infinite coaxial cable and will provide an approximation of the condition at Γ_{coax}, where V is the potential difference inside the coaxial cable. Expression (3e) represents the relation between the magnetic field and the current I inside the coaxial cable (Ampere's law). Expression (3f) is an artificial boundary condition used to approximate the far-field condition for the case when equation (3a) and equation (3b) are solved in the upper half space. Condition (3f) sets the incoming so-called characteristic variable to a value $\boldsymbol{W}^-$, which can be used to model for entrance of an incoming plane wave. The left-hand side of expression (3g) represents a signal propagates inside the coaxial cable in the positive z direction, where $Z_{\text{c}} = Z_{\text{m}}\kappa$ is the coaxial cable intrinsic impedance with $Z_{\text{m}} = \sqrt{\mu/\epsilon}$ and $\kappa = \log\frac{b}{a}/2\pi$, and $g(t)$ is a time domain signal that cover the frequency band of interest. We use the boundary at Γ_{coax} to impose the signal $g(t)$. Moreover, inside the coaxial cable the term $V - Z_{\text{c}} I$ represents a signal that propagates in the negative z direction [11].

We formulate an objective function that represents the outgoing energy in the coaxial as

$$W_{\text{out,coax}} = \frac{1}{4Z_{\text{c}}}\int_0^T (V - Z_{\text{c}} I)^2\, dt, \tag{4}$$

where T denotes the length of the observation time interval.

3. CONTINUOUS SENSITIVITY ANALYSIS

We need an expression for the derivatives of $W_{\text{out,coax}}$ with respect to changes in the conductivity distribution $\sigma(\boldsymbol{x})$ inside the domain Ω. Let $\delta\sigma$ be a perturbation of the conductivity σ. The directional derivative of $W_{\text{out,coax}}$ is defined as [12],

$$\delta W_{\text{out,coax}}(\sigma; \delta\sigma) = \lim_{s \to 0} \frac{W_{\text{out,coax}}(\sigma + s\,\delta\sigma) - W_{\text{out,coax}}(\sigma)}{s}. \tag{5}$$

We will derive an integral expression for the directional derivative, where the integrand is linear in $\delta\sigma$. We start by differentiating the objective function (4) to obtain

$$\delta W_{\text{out,coax}} = \frac{1}{2Z_{\text{c}}} \int_0^T (\delta V - Z_{\text{c}}\,\delta I)(V - Z_{\text{c}} I)\, dt, \tag{6}$$

where δI and δV are the first-order variations of the current and the potential difference inside the coaxial cable, respectively. To find an explicit relation between $\delta W_{\text{out,coax}}$ and $\delta\sigma$, we need to know how δI and δV depend on $\delta\sigma$. We depend on the system governing equations (3). By differentiating system (3) with respect to the design variation $\delta\sigma$, we obtain

$$\frac{\partial}{\partial t}\mu\,\delta \boldsymbol{H} + \nabla\times\delta\boldsymbol{E} = \boldsymbol{0} \qquad \text{in } \Omega_\infty, \text{ for } t>0, \tag{7a}$$

$$\frac{\partial}{\partial t}\epsilon\,\delta \boldsymbol{E} + \sigma\,\delta\boldsymbol{E} + \delta\sigma\,\boldsymbol{E} - \nabla\times\delta\boldsymbol{H} = \boldsymbol{0} \qquad \text{in } \Omega_\infty, \text{ for } t>0, \tag{7b}$$

$$\boldsymbol{n}\times\delta\boldsymbol{E} = \boldsymbol{0} \qquad \text{on } \Gamma_0, \text{ for } t>0, \tag{7c}$$

$$\delta\boldsymbol{E}_t = \frac{\delta V}{\log b/a}\frac{\boldsymbol{x}-\boldsymbol{x}_{\text{c}}}{|\boldsymbol{x}-\boldsymbol{x}_{\text{c}}|^2} \qquad \boldsymbol{x}\in\Gamma_{\text{coax}}, \text{ for } t>0, \tag{7d}$$

$$\delta I = \int_{C_r}\delta\boldsymbol{H}\cdot d\boldsymbol{l} \qquad C_r\subset\Gamma_{\text{coax}}, \text{ for } t>0, \tag{7e}$$

$$\delta\boldsymbol{E}_t + Z_0\,\boldsymbol{n}\times\delta\boldsymbol{H} = \boldsymbol{0} \qquad \text{on } \Gamma_{\text{out}}, \text{ for } t>0, \tag{7f}$$

$$\delta V + Z_{\text{c}}\,\delta I = 0 \qquad \text{on } \Gamma_{\text{coax}}, \text{ for } t>0, \tag{7g}$$

$$\delta\boldsymbol{E}|_{t=0} = \boldsymbol{0}, \tag{7h}$$

$$\delta\boldsymbol{H}|_{t=0} = \boldsymbol{0}. \tag{7i}$$

We introduce the field vectors $\boldsymbol{H}^*$ and $\boldsymbol{E}^*$, perform the scalar product of $\boldsymbol{H}^*$ and $\boldsymbol{E}^*$ with equation (7a) and (7b), respectively, then integrate over the time interval $(0,T)$ and the domain Ω_∞ to obtain

$$\begin{aligned}\int_{\Omega_\infty}\int_0^T \Big(\boldsymbol{H}^*\cdot\frac{\partial}{\partial t}(\mu\,\delta\boldsymbol{H}) + \boldsymbol{H}^*\cdot\nabla\times\delta\boldsymbol{E} + \boldsymbol{E}^*\cdot\frac{\partial}{\partial t}(\epsilon\,\delta\boldsymbol{E})\\ + \sigma\,\delta\boldsymbol{E}\cdot\boldsymbol{E}^* + \delta\sigma\,\boldsymbol{E}\cdot\boldsymbol{E}^* - \boldsymbol{E}^*\cdot\nabla\times\delta\boldsymbol{H}\Big) = \boldsymbol{0}.\end{aligned} \tag{8}$$

Consider the second and the last terms in equation (8), we apply integration by parts for the domain integrals

$$\begin{aligned}\int_{\Omega_\infty}\int_0^T \Big(\boldsymbol{H}^*\cdot\nabla\times\delta\boldsymbol{E} - \boldsymbol{E}^*\cdot\nabla\times\delta\boldsymbol{H}\Big) = \int_{\partial\Omega_\infty}\int_0^T (\boldsymbol{n}\times\delta\boldsymbol{E})\cdot\boldsymbol{H}_t^*\\ + \int_{\Omega_\infty}\int_0^T \delta\boldsymbol{E}\cdot\nabla\times\boldsymbol{H}^* - \int_{\partial\Omega_\infty}\int_0^T (\boldsymbol{n}\times\delta\boldsymbol{H})\cdot\boldsymbol{E}_t^* - \int_{\Omega_\infty}\int_0^T \delta\boldsymbol{H}\cdot\nabla\times\boldsymbol{E}^*.\end{aligned} \tag{9}$$

In the right side of equation (9), the first integral over $\partial\Omega_\infty$ can be written as

$$\begin{aligned}\int_{\partial\Omega_\infty}\int_0^T (\boldsymbol{n}\times\delta\boldsymbol{E})\cdot\boldsymbol{H}_t^* = -\int_{\partial\Omega_\infty}\int_0^T (\boldsymbol{n}\times\boldsymbol{H}^*)\cdot\delta\boldsymbol{E}_t\\ = -\int_{\Gamma_{\text{coax}}}\int_0^T (\boldsymbol{n}\times\boldsymbol{H}^*)\cdot\delta\boldsymbol{E}_t + \int_{\Gamma_0}\int_0^T (\boldsymbol{n}\times\delta\boldsymbol{E})\cdot\boldsymbol{H}_t^* - \int_{\Gamma_{\text{out}}}\int_0^T (\boldsymbol{n}\times\boldsymbol{H}^*)\cdot\delta\boldsymbol{E}_t.\end{aligned} \tag{10}$$

By using expressions (7c) and (7d) in the last equation, we can write

$$\begin{aligned}
&\int_{\partial\Omega_\infty}\int_0^T (\boldsymbol{n}\times\delta\boldsymbol{E})\cdot\boldsymbol{H}_t^* \\
&\quad= -\int_{\Gamma_{\mathrm{coax}}}\int_0^T \frac{\delta V}{\log b/a}(\boldsymbol{n}\times\boldsymbol{H}^*)\cdot\frac{\boldsymbol{x}-\boldsymbol{x}_{\mathrm{c}}}{|\boldsymbol{x}-\boldsymbol{x}_{\mathrm{c}}|^2} - \int_{\Gamma_{\mathrm{out}}}\int_0^T (\boldsymbol{n}\times\boldsymbol{H}^*)\cdot\delta\boldsymbol{E}_t \\
&\quad= -\int_a^b\int_{C_r}\int_0^T \frac{\delta V}{\log b/a}\boldsymbol{H}^*\cdot d\boldsymbol{l}\frac{1}{r}dr - \int_{\Gamma_{\mathrm{out}}}\int_0^T (\boldsymbol{n}\times\boldsymbol{H}^*)\cdot\delta\boldsymbol{E}_t \\
&\quad= -\int_0^T \delta V\, I^* - \int_{\Gamma_{\mathrm{out}}}\int_0^T (\boldsymbol{n}\times\boldsymbol{H}^*)\cdot\delta\boldsymbol{E}_t,
\end{aligned} \tag{11}$$

where

$$I^* = \int_{C_r} \boldsymbol{H}^*\cdot d\boldsymbol{l}. \tag{12}$$

Similarly, we evaluate the second integral over $\partial\Omega_\infty$ in the right-hand side of expression (9),

$$\begin{aligned}
&-\int_{\partial\Omega_\infty}\int_0^T (\boldsymbol{n}\times\delta\boldsymbol{H})\cdot\boldsymbol{E}_t^* \\
&\quad= -\int_{\Gamma_{\mathrm{coax}}}\int_0^T (\boldsymbol{n}\times\delta\boldsymbol{H})\cdot\boldsymbol{E}_t^* + \int_{\Gamma_0}\int_0^T (\boldsymbol{n}\times\boldsymbol{E}^*)\cdot\delta\boldsymbol{H}_t - \int_{\Gamma_{\mathrm{out}}}\int_0^T (\boldsymbol{n}\times\delta\boldsymbol{H})\cdot\boldsymbol{E}_t^* \\
&\quad= -\int_{\Gamma_{\mathrm{coax}}}\int_0^T (\boldsymbol{n}\times\delta\boldsymbol{H})\cdot\boldsymbol{E}_t^* + \int_{\Gamma_0}\int_0^T (\boldsymbol{n}\times\boldsymbol{E}^*)\cdot\delta\boldsymbol{H}_t + \frac{1}{Z_0}\int_{\Gamma_{\mathrm{out}}}\int_0^T \delta\boldsymbol{E}_{\mathrm{t}}\cdot\boldsymbol{E}_t^*,
\end{aligned} \tag{13}$$

where expression (7f) is used to substitute the third term. Substituting equations (11) and (13) back into equation (9), equation (9) back into equation (8), and rearranging the terms, we obtain

$$\begin{aligned}
&\int_{\Omega_\infty}\int_0^T \boldsymbol{H}^*\cdot\frac{\partial}{\partial t}(\mu\,\delta\boldsymbol{H}) + \int_{\Omega_\infty}\int_0^T \boldsymbol{E}^*\cdot\frac{\partial}{\partial t}(\epsilon\,\delta\boldsymbol{E}) + \int_{\Omega_\infty}\int_0^T \sigma\,\delta\boldsymbol{E}\cdot\boldsymbol{E}^* \\
&\quad+ \int_{\Omega}\int_0^T \delta\sigma\,\boldsymbol{E}\cdot\boldsymbol{E}^* + \int_{\Gamma_0}\int_0^T \delta\boldsymbol{H}_t\cdot(\boldsymbol{n}\times\boldsymbol{E}^*) + \frac{1}{Z_0}\int_{\Gamma_{\mathrm{out}}}\int_0^T \delta\boldsymbol{E}_{\mathrm{t}}\cdot(\boldsymbol{E}_t^* - Z_0\,\boldsymbol{n}\times\boldsymbol{H}^*) \\
&\quad+ \int_{\Omega_\infty}\int_0^T \delta\boldsymbol{E}\cdot\nabla\times\boldsymbol{H}^* - \int_{\Omega_\infty}\int_0^T \delta\boldsymbol{H}\cdot\nabla\times\boldsymbol{E}^* - \int_{\Gamma_{\mathrm{coax}}}\int_0^T (\boldsymbol{n}\times\delta\boldsymbol{H})\cdot\boldsymbol{E}_t^* - \int_0^T \delta V\, I^* = \boldsymbol{0}.
\end{aligned} \tag{14}$$

Applying integration by parts on the time integrals of the first two terms in equation (14), we obtain

$$\begin{aligned}
&\int_{\Omega_\infty}\mu\,\delta\boldsymbol{H}(T)\cdot\boldsymbol{H}^*(T) - \int_{\Omega_\infty}\int_0^T \delta\boldsymbol{H}\cdot\frac{\partial}{\partial t}\left(\mu\boldsymbol{H}^*\right) + \int_{\Omega_\infty}\epsilon\,\delta\boldsymbol{E}(T)\cdot\boldsymbol{E}^*(T) \\
&\quad- \int_{\Omega_\infty}\int_0^T \delta\boldsymbol{E}\cdot\frac{\partial}{\partial t}(\epsilon\boldsymbol{E}^*) + \int_{\Omega_\infty}\int_0^T \sigma\,\delta\boldsymbol{E}\cdot\boldsymbol{E}^* + \int_{\Omega}\int_0^T \delta\sigma\,\boldsymbol{E}\cdot\boldsymbol{E}^* \\
&\quad+ \int_{\Gamma_0}\int_0^T \delta\boldsymbol{H}_t\cdot(\boldsymbol{n}\times\boldsymbol{E}^*) + \int_{\Omega_\infty}\int_0^T \delta\boldsymbol{E}\cdot\nabla\times\boldsymbol{H}^* - \int_{\Omega_\infty}\int_0^T \delta\boldsymbol{H}\cdot\nabla\times\boldsymbol{E}^* \\
&\quad+ \frac{1}{Z_0}\int_{\Gamma_{\mathrm{out}}}\int_0^T \delta\boldsymbol{E}_{\mathrm{t}}\cdot(\boldsymbol{E}_t^* - Z_0\,\boldsymbol{n}\times\boldsymbol{H}^*) - \int_{\Gamma_{\mathrm{coax}}}\int_0^T (\boldsymbol{n}\times\delta\boldsymbol{H})\cdot\boldsymbol{E}_t^* - \int_0^T \delta V\, I^* = \boldsymbol{0}.
\end{aligned} \tag{15}$$

Rearranging the terms in equation (15) gives

$$\begin{aligned}
&\int_{\Omega_\infty}\int_0^T \delta\boldsymbol{H}\cdot\Big(-\frac{\partial}{\partial t}(\mu\boldsymbol{H}^*)-\nabla\times\boldsymbol{E}^*\Big)\\
&+\int_{\Omega_\infty}\int_0^T \delta\boldsymbol{E}\cdot\Big(-\frac{\partial}{\partial t}(\epsilon\boldsymbol{E}^*)+\sigma\boldsymbol{E}^*+\nabla\times\boldsymbol{H}^*\Big)+\int_{\Gamma_0}\int_0^T \delta\boldsymbol{H}_t\cdot(\boldsymbol{n}\times\boldsymbol{E}^*)\\
&+\int_{\Omega}\int_0^T \delta\sigma\,\boldsymbol{E}\cdot\boldsymbol{E}^*+\frac{1}{Z_0}\int_{\Gamma_{\text{out}}}\int_0^T \delta\boldsymbol{E}_{\text{t}}\cdot(\boldsymbol{E}_t^*-Z_0\,\boldsymbol{n}\times\boldsymbol{H}^*)\\
&+\int_{\Omega_\infty}\epsilon\,\delta\boldsymbol{E}(T)\cdot\boldsymbol{E}^*(T)+\int_{\Omega_\infty}\mu\,\delta\boldsymbol{H}(T)\cdot\boldsymbol{H}^*(T)-\int_{\Gamma_{\text{coax}}}\int_0^T(\boldsymbol{n}\times\delta\boldsymbol{H})\cdot\boldsymbol{E}_t^*\\
&-\int_0^T \delta V\,I^*=\boldsymbol{0}.
\end{aligned}\tag{16}$$

We now require that $\boldsymbol{E}^*$ and $\boldsymbol{H}^*$ to satisfy

$$\begin{aligned}
&-\frac{\partial}{\partial t}(\mu\boldsymbol{H}^*)-\nabla\times\boldsymbol{E}^*=\boldsymbol{0} && \text{in } \Omega_\infty\text{, for } t>0, && \text{(17a)}\\
&-\frac{\partial}{\partial t}(\epsilon\boldsymbol{E}^*)+\sigma\boldsymbol{E}^*+\nabla\times\boldsymbol{H}^*=\boldsymbol{0} && \text{in } \Omega_\infty\text{, for } t>0, && \text{(17b)}\\
&\boldsymbol{n}\times\boldsymbol{E}^*=\boldsymbol{0} && \text{on } \Gamma_0\text{, for } t>0, && \text{(17c)}\\
&\boldsymbol{E}_t^*=\frac{V^*}{\log b/a}\frac{\boldsymbol{x}-\boldsymbol{x}_{\text{c}}}{|\boldsymbol{x}-\boldsymbol{x}_{\text{c}}|^2} && \boldsymbol{x}\in\Gamma_{\text{coax}}\text{, for } t>0, && \text{(17d)}\\
&\boldsymbol{E}_t^*-Z_0\,\boldsymbol{n}\times\boldsymbol{H}^*=\boldsymbol{0} && \text{on } \Gamma_{\text{out}}\text{, for } t>0, && \text{(17e)}\\
&\boldsymbol{H}^*(T)=\boldsymbol{E}^*(T)=\boldsymbol{0}, && && \text{(17f)}
\end{aligned}$$

where V^* is a given scalar function of time, specified below. Then equation (16) reduces to

$$\int_{\Omega}\int_0^T \delta\sigma\,\boldsymbol{E}\cdot\boldsymbol{E}^*=\frac{1}{\log b/a}\int_{\Gamma_{\text{coax}}}\int_0^T(\boldsymbol{n}\times\delta\boldsymbol{H})\cdot\frac{\boldsymbol{x}-\boldsymbol{x}_{\text{c}}}{|\boldsymbol{x}-\boldsymbol{x}_{\text{c}}|^2}V^*+\int_0^T \delta V\,I^*.\tag{18}$$

By using expression (17d), the first integral in the right-hand side of equation (18) can be written in terms of the current and potential difference (similar to expression (11)). Thus, we obtain

$$\int_{\Omega}\int_0^T \delta\sigma\,\boldsymbol{E}\cdot\boldsymbol{E}^*=\int_0^T V^*\,\delta I+\int_0^T \delta V\,I^*.\tag{19}$$

We substitute $\delta V=-\delta I\;Z_{\text{c}}$ (from equation (7g)) into equation (19) to obtain

$$\begin{aligned}
\int_{\Omega}\int_0^T \delta\sigma\,\boldsymbol{E}\cdot\boldsymbol{E}^*&=\int_0^T \delta I\Big(V^*-Z_{\text{c}}I^*\Big)\\
&=-\int_0^T \frac{1}{2Z_{\text{c}}}\Big(\delta V-Z_{\text{c}}\delta I\Big)\Big(V^*-Z_{\text{c}}I^*\Big).
\end{aligned}\tag{20}$$

Now we require that

$$V^*-Z_{\text{c}}I^*=V-Z_{\text{c}}I,\qquad \text{for } t>0.\tag{21}$$

Then by using expression (6), expression (20) can be written as

$$\delta W_{\text{out,coax}}=-\int_{\Omega}\int_0^T \boldsymbol{E}\cdot\boldsymbol{E}^*\,\delta\sigma.\tag{22}$$

Expression (22) represents the directional derivative of the objective function (4) when the conductivity is perturbed by $\delta\sigma$, given in terms of the adjoint-field $\boldsymbol{E}^*$, which requires the solution of an adjoint-field problem summarized by

$$
\begin{aligned}
&-\frac{\partial}{\partial t}(\mu \boldsymbol{H}^*) - \nabla\times\boldsymbol{E}^* = \boldsymbol{0} && \text{in } \Omega_\infty, \text{ for } t>0, && \text{(23a)}\\
&-\frac{\partial}{\partial t}(\epsilon \boldsymbol{E}^*) + \sigma\boldsymbol{E}^* + \nabla\times\boldsymbol{H}^* = \boldsymbol{0} && \text{in } \Omega_\infty, \text{ for } t>0, && \text{(23b)}\\
&\boldsymbol{n}\times\boldsymbol{E}^* = \boldsymbol{0} && \text{on } \Gamma_0, \text{ for } t>0, && \text{(23c)}\\
&\boldsymbol{E}_t^* - Z_0\,\boldsymbol{n}\times\boldsymbol{H}^* = \boldsymbol{0} && \text{on } \Gamma_{\text{out}}, \text{ for } t>0, && \text{(23d)}\\
&\boldsymbol{E}_t^* = \frac{V^*}{\log b/a}\frac{\boldsymbol{x}-\boldsymbol{x}_\text{c}}{|\boldsymbol{x}-\boldsymbol{x}_\text{c}|^2} && \boldsymbol{x}\in\Gamma_{\text{coax}}, \text{ for } t>0, && \text{(23e)}\\
&I^* = \int_{C_r}\boldsymbol{H}^*\cdot d\boldsymbol{l} && C_r\subset\Gamma_{\text{coax}}, \text{ for } t>0, && \text{(23f)}\\
&V^* - Z_\text{c}I^* = V - Z_\text{c}I && \text{on } \Gamma_{\text{coax}}, \text{ for } t>0, && \text{(23g)}\\
&\boldsymbol{E}^*|_{t=T} = \boldsymbol{0}, && && \text{(23h)}\\
&\boldsymbol{H}^*|_{t=T} = \boldsymbol{0}. && && \text{(23i)}
\end{aligned}
$$

System (23) represents a terminal value problem ($\boldsymbol{E}^*|_{t=T}$ and $\boldsymbol{H}^*|_{t=T}$ are specified), which by the change of variable $\tau = T - t$ can be changed to an initial value problem and for consistency we change the sign of the magnetic field $\boldsymbol{H}^*$ (i.e. to preserve the correct direction of the Poynting vector). Then the adjoint-field problem can be written as

$$
\begin{aligned}
&\frac{\partial}{\partial \tau}(\mu \boldsymbol{H}^*) + \nabla\times\boldsymbol{E}^* = \boldsymbol{0} && \text{in } \Omega_\infty, \text{ for } \tau>0, && \text{(24a)}\\
&\frac{\partial}{\partial \tau}(\epsilon \boldsymbol{E}^*) + \sigma\boldsymbol{E}^* - \nabla\times\boldsymbol{H}^* = \boldsymbol{0} && \text{in } \Omega_\infty, \text{ for } \tau>0, && \text{(24b)}\\
&\boldsymbol{n}\times\boldsymbol{E}^* = \boldsymbol{0} && \text{on } \Gamma_0, \text{ for } \tau>0, && \text{(24c)}\\
&\boldsymbol{E}_t^* + Z_0\,\boldsymbol{n}\times\boldsymbol{H}^* = \boldsymbol{0} && \text{on } \Gamma_{\text{out}}, \text{ for } \tau>0, && \text{(24d)}\\
&\boldsymbol{E}_t^* = \frac{V^*}{\log b/a}\frac{\boldsymbol{x}-\boldsymbol{x}_\text{c}}{|\boldsymbol{x}-\boldsymbol{x}_\text{c}|^2} && \boldsymbol{x}\in\Gamma_{\text{coax}}, \text{ for } \tau>0, && \text{(24e)}\\
&I^*(\tau) = -I^*(t) = -\int_{C_r}\boldsymbol{H}^*\cdot d\boldsymbol{l} && C_r\subset\Gamma_{\text{coax}}, \text{ for } \tau>0, && \text{(24f)}\\
&V^*(\tau) + Z_\text{c}I^*(\tau) = V(T-\tau) - Z_\text{c}I(T-\tau), && \text{for } \tau>0, && \text{(24g)}\\
&\boldsymbol{E}^*|_{\tau=0} = \boldsymbol{0}, && && \text{(24h)}\\
&\boldsymbol{H}^*|_{\tau=0} = \boldsymbol{0}. && && \text{(24i)}
\end{aligned}
$$

The derived adjoint system (24) only differs from the forward system (3) in the excitation expression (24g). For the adjoint system, the incoming signal inside the coaxial cable is given as the time reversal of the outgoing signal inside the coaxial cable of the forward problem. The final expression of the directional derivative of the objective function (4) when the conductivity is perturbed by $\delta\sigma$ can be written as

$$\delta W_{\text{out,coax}} = -\int_\Omega\int_0^T \boldsymbol{E}(T-\tau)\cdot\boldsymbol{E}^*(\tau)\,\delta\sigma. \tag{25}$$

The Gâteaux derivatives [12] of the objective function (4) with respect to the conductivity distribution σ can be identified as the integral kernel

$$GW_{\text{out,coax}}(\sigma;\boldsymbol{x}) = -\int_0^T \boldsymbol{E}(T-\tau,\boldsymbol{x})\cdot\boldsymbol{E}^*(\tau,\boldsymbol{x}). \tag{26}$$

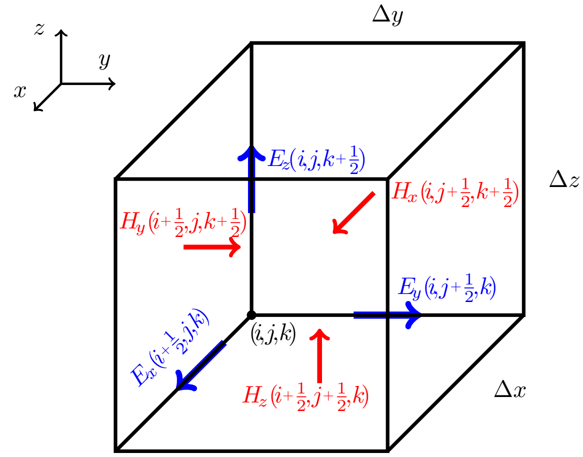

Figure 2. The distribution of the electric and magnetic fields in the basic Yee cell.

4. DISCRETE SENSITIVITY ANALYSIS BASED ON THE FDTD METHOD

In this section we introduce numerical approximations for solving problem (3) by the FDTD method [13–15]. We start by briefly reviewing the FDTD method, introducing an equivalent discrete objective function, then we derive the derivative expression in the discrete case.

4.1. FDTD method

The FDTD method is one of the most commonly used numerical methods to solve the time-domain Maxwell's equations. The FDTD method discretizes the computational domain into small cubical cells, called Yee cells. For each cell, the six field components are located to match the curl operators in Maxwell's equations. Figure 2 shows the Yee cell for a cube (i, j, k) with dimensions Δx, Δy, and Δz. The electric field components are located centered and along the cell edges, while the magnetic field components are located centered and normal to the cell faces. Objects are directly represented in the Yee grid by their constitutive parameters. The conductivity and the permittivity have the same spatial distribution as the discrete electric field, and the permeability has the spatial distribution of the discrete magnetic field.

We use the uniaxial perfectly matched layer (UPML) to simulate the open space radiation condition [16]. By considering a region of space that is source free but may have a medium with variable material properties, Maxwell's equations with the UPML parameters included can be written as [14],

$$\left(\frac{\partial}{\partial t} + \sigma^{p_2}\right) \boldsymbol{B} + \frac{1}{\mu}\nabla \times \boldsymbol{E} = \boldsymbol{0}, \tag{27a}$$

$$\left(\frac{\partial}{\partial t} + \sigma^{p_3}\right) \boldsymbol{H} - (\frac{\partial}{\partial t} + \sigma^{p_1})\boldsymbol{B} = \boldsymbol{0}, \tag{27b}$$

$$\left(\frac{\partial}{\partial t} + \frac{\sigma}{\epsilon}\right) \boldsymbol{P} - \frac{1}{\epsilon}\nabla \times \boldsymbol{H} = \boldsymbol{0}, \tag{27c}$$

$$\left(\frac{\partial}{\partial t} + \sigma^{p_3}\right) \boldsymbol{Q} - \frac{\partial}{\partial t}\boldsymbol{P} = \boldsymbol{0}, \tag{27d}$$

$$\left(\frac{\partial}{\partial t} + \sigma^{p_2}\right) \boldsymbol{E} - \left(\frac{\partial}{\partial t} + \sigma^{p_1}\right) \boldsymbol{Q} = \boldsymbol{0}, \tag{27e}$$

with,

$$\begin{aligned}\sigma^{p_1} &= \mathrm{diag}(\sigma_x^p/\epsilon_0,\ \sigma_y^p/\epsilon_0,\ \sigma_z^p/\epsilon_0),\\ \sigma^{p_2} &= \mathrm{diag}(\sigma_y^p/\epsilon_0,\ \sigma_z^p/\epsilon_0,\ \sigma_x^p/\epsilon_0),\\ \sigma^{p_3} &= \mathrm{diag}(\sigma_z^p/\epsilon_0,\ \sigma_x^p/\epsilon_0,\ \sigma_y^p/\epsilon_0),\end{aligned} \tag{28}$$

where μ, ϵ, and σ are the permeability, permittivity, and conductivity of the medium, respectively; μ_0 and ϵ_0 are the permeability and permittivity of vacuum; σ_x^p, σ_y^p, and σ_z^p represent fictitious conductivities that have nonzero values only inside the UPML layer; $\boldsymbol{E}$ and $\boldsymbol{H}$ are the primal electric and magnetic field vectors; and $\boldsymbol{P}$, $\boldsymbol{Q}$, and $\boldsymbol{B}$ are auxiliary field vectors that are used for the numerical implementation of the UPML. Note that, $\boldsymbol{P}$ and $\boldsymbol{Q}$ are associated with the electric field vector $\boldsymbol{E}$, and $\boldsymbol{B}$ is associated with the magnetic field vector $\boldsymbol{H}$. In the PML-free region, all σ_i^p are zeros, the auxiliary field vectors are not used, and equations (27) reduce to Maxwell's equations in free space (3a–3b).

In Cartesian coordinates, Maxwell's equations can be written in a compact form as follow

$$\frac{\partial}{\partial t}B_{x,y,z} + \frac{\sigma^p_{y,z,x}}{\epsilon_0}B_{x,y,z} + \frac{1}{\mu_{x,y,z}}\left[\frac{\partial}{\partial_{y,z,x}}E_{z,x,y} - \frac{\partial}{\partial_{z,x,y}}E_{y,z,x}\right] = \mathbf{0}, \tag{29a}$$

$$\frac{\partial}{\partial t}H_{x,y,z} + \frac{\sigma^p_{z,x,y}}{\epsilon_0}H_{x,y,z} - \frac{\partial}{\partial t}B_{x,y,z} - \frac{\sigma_{x,y,z}}{\epsilon_0}B_{x,y,z} = \mathbf{0}, \tag{29b}$$

$$\frac{\partial}{\partial t}P_{x,y,z} + \frac{\sigma_{x,y,z}}{\epsilon_{x,y,z}}P_{x,y,z} - \frac{1}{\epsilon_{x,y,z}}\left[\frac{\partial}{\partial_{y,z,x}}H_{z,x,y} - \frac{\partial}{\partial_{z,x,y}}H_{y,z,x}\right] = \mathbf{0}, \tag{29c}$$

$$\frac{\partial}{\partial t}Q_{x,y,z} + \frac{\sigma^p_{z,x,y}}{\epsilon_0}Q_{x,y,z} - \frac{\partial}{\partial t}P_{x,y,z} = \mathbf{0}, \tag{29d}$$

$$\frac{\partial}{\partial t}E_{x,y,z} + \frac{\sigma^p_{y,z,x}}{\epsilon_0}E_{x,y,z} - \frac{\partial}{\partial t}Q_{x,y,z} - \frac{\sigma^p_{x,y,z}}{\epsilon_0}Q_{x,y,z} = \mathbf{0}, \tag{29e}$$

where each line in equations (29) represents three equations, that is, one equation for each corresponding Cartesian suffix. For example, if we consider the first suffix in equation (29a), we obtain the equation

$$\frac{\partial}{\partial t}B_x + \frac{\sigma_y^p}{\epsilon_0}B_x + \frac{1}{\mu_x}\left[\frac{\partial}{\partial_y}E_z - \frac{\partial}{\partial_z}E_y\right] = \mathbf{0}. \tag{30}$$

For the discrete sensitivity analysis, we apply the FDTD discretization to equations (29). To represent the discrete equations in a compact manner, we use the central finite difference operators

$$D_xU = \frac{U^n(\hat{i}+\frac{1}{2},\hat{j},\hat{k}) - U^n(\hat{i}-\frac{1}{2},\hat{j},\hat{k})}{\Delta x}, \tag{31a}$$

$$D_yU = \frac{U^n(\hat{i},\hat{j}+\frac{1}{2},k) - U^n(\hat{i},\hat{j}-\frac{1}{2},\hat{k})}{\Delta y}, \tag{31b}$$

$$D_zU = \frac{U^n(\hat{i},\hat{j},k+\frac{1}{2}) - U^n(\hat{i},\hat{j},\hat{k}-\frac{1}{2})}{\Delta z}, \tag{31c}$$

$$D_tU = \frac{U^{n+\frac{1}{2}}(\hat{i},\hat{j},\hat{k}) - U^{n-\frac{1}{2}}(\hat{i},\hat{j},\hat{k})}{\Delta t}, \tag{31d}$$

and the time average operator

$$S_tU = \frac{U^{n+\frac{1}{2}}(\hat{i},\hat{j},\hat{k}) + U^{n-\frac{1}{2}}(\hat{i},\hat{j},\hat{k})}{2}, \tag{32a}$$

where Δt is the time step used in the FDTD method and U denotes any of the field components in Maxwell's equations, for which we need to approximate the partial derivative at point $(\hat{i},\hat{j},\hat{k})$ in terms of the discrete fields in a Yee cell. For example, in equation (30) we need to approximate the spatial derivative of the E_z with respect to the y coordinate at the point $(\hat{i}, \hat{j}, \hat{k}) \equiv (i, j + \frac{1}{2}, k + \frac{1}{2})$ (i.e., at the location of B_x in the Yee cell). Then, we use the components of E_z at $(\hat{i}, \hat{j} + \frac{1}{2}, \hat{k}) \equiv (i, j + 1, k + \frac{1}{2})$ and at $(\hat{i}, \hat{j} - \frac{1}{2}, \hat{k}) \equiv (i, j, k + \frac{1}{2})$.

We consider the solution of equations (29) over an analysis domain $\Omega^\Delta_\infty = \Omega^\Delta \cup \Gamma^\Delta_{\text{coax}}$, where Ω^Δ denotes a cubical grid and $\Gamma^\Delta_{\text{coax}}$ denotes a discrete coaxial cable modelled with four Yee cells and connected to the cubical grid, as will be shown the next section. Excluding the intersection with the coaxial cable $\Gamma^\Delta_{\text{coax}}$, the outer boundaries of the cubical grid, $\partial\Omega^\Delta$, is assumed to be a perfect electric conductor, which implies the boundary conditions

$$P^n_t = Q^n_t = E^n_t = \mathbf{0} \qquad \text{on} \quad \partial\Omega^\Delta \setminus \partial\Gamma^\Delta_{\text{coax}}, \quad \text{for } n = 0, \ldots, N, \tag{33}$$

where P_t, Q_t, and E_t denote edge components residing on $\partial\Omega^\Delta$, and N is the total number of time steps used in the FDTD simulation. Applying the finite difference approximation to the spatial and temporal derivatives in equations (29), and setting the discrete electric and magnetic fields at full and half time indexes (leapfrog scheme), respectively, the standard FDTD update equations can be written as

$$\left[D_t B_{x,y,z} + \frac{\sigma^p_{y,z,x}}{\epsilon_0} S_t B_{x,y,z} + \frac{1}{\mu_{x,y,z}} \big(D_{y,z,x} E_{z,x,y} - D_{z,x,y} E_{y,z,x} \big) \right] \Big|^n = \mathbf{0}, \tag{34a}$$

$$\left[D_t H_{x,y,z} + \frac{\sigma^p_{z,x,y}}{\epsilon_0} S_t H_{x,y,z} - D_t B_{x,y,z} - \frac{\sigma^p_{x,y,z}}{\epsilon_0} S_t B_{x,y,z} \right] \Big|^n = \mathbf{0}, \tag{34b}$$

$$\left[D_t P_{x,y,z} + \frac{\sigma_{x,y,z}}{\epsilon_{x,y,z}} S_t P_{x,y,z} - \frac{1}{\epsilon_{x,y,z}} \big(D_{y,z,x} H_{z,x,y} - D_{z,x,y} H_{y,z,x} \big) \right] \Big|^{n+\frac{1}{2}} = \mathbf{0}, \tag{34c}$$

$$\left[D_t Q_{x,y,z} + \frac{\sigma^p_{z,x,y}}{\epsilon_0} S_t Q_{x,y,z} - D_t P_{x,y,z} \right] \Big|^{n+\frac{1}{2}} = \mathbf{0}, \tag{34d}$$

$$\left[D_t E_{x,y,z} + \frac{\sigma^p_{y,z,x}}{\epsilon_0} S_t E_{x,y,z} - D_t Q_{x,y,z} - \frac{\sigma^p_{x,y,z}}{\epsilon_0} S_t Q_{x,y,z} \right] \Big|^{n+\frac{1}{2}} = \mathbf{0}, \tag{34e}$$

and we assume an initial condition

$$B^{-\frac{1}{2}}_{x,y,z} = H^{-\frac{1}{2}}_{x,y,z} = P^0_{x,y,z} = Q^0_{x,y,z} = E^0_{x,y,z} = \mathbf{0}. \tag{35}$$

To clarify the notation, if we expand the equation corresponding to the first subscript index in equations (34a) we obtain the FDTD update equation

$$\begin{aligned} B^{n+\frac{1}{2}}_x(i, j + \tfrac{1}{2}, k + \tfrac{1}{2}) &= C_1 B^{n-\frac{1}{2}}_x(i, j + \tfrac{1}{2}, k + \tfrac{1}{2}) + C_2 \big[E^n_z(i, j + 1, k + \tfrac{1}{2}) \\ &\quad - E^n_z(i, j, k + \tfrac{1}{2}) \big] + C_3 \big[E^n_y(i, j + \tfrac{1}{2}, k + 1) - E^n_y(i, j + \tfrac{1}{2}, k) \big], \end{aligned} \tag{36}$$

where

$$\begin{aligned} C_1 &= \frac{1/\Delta t - \sigma^p_y(i, j + \frac{1}{2}, k + \frac{1}{2})/2\epsilon_0}{1/\Delta t + \sigma^p_y(i, j + \frac{1}{2}, k + \frac{1}{2})/2\epsilon_0}, \\ C_2 &= -\frac{1/\Delta y}{\mu/\Delta t + \mu\sigma^p_y(i, j + \frac{1}{2}, k + \frac{1}{2})/2\epsilon_0}, \\ C_3 &= \frac{1/\Delta z}{\mu/\Delta t + \mu\sigma^p_y(i, j + \frac{1}{2}, k + \frac{1}{2})/2\epsilon_0}. \end{aligned}$$

4.2. Discrete coaxial cable model and objective function

In reference [11], we proposed a model for a coaxial cable that can be used with the FDTD method. The model is based on four Yee cells that are located one cell below the ground plane, as shown in Figure 3. The outer eight vertical faces of the four cells represent the outer shield of the coaxial cable, while the shared edge at the center represents the inner probe. We denote these four Yee cells by $\Gamma^\Delta_{\text{coax}}$. Inside the coaxial cable we can set a signal

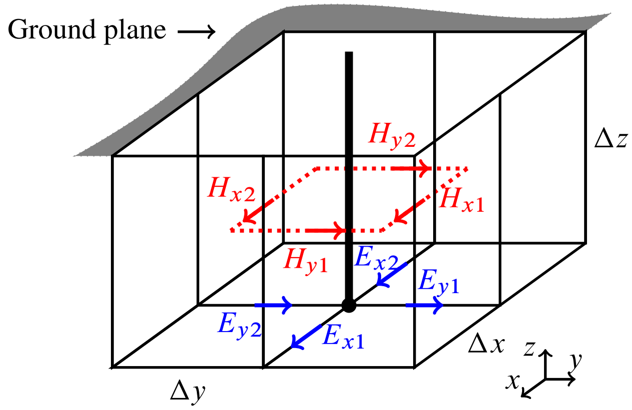

Figure 3. The domain $\Gamma^{\Delta}_{\text{coax}}$ holds four neighbouring Yee cells to model a z directed discrete coaxial cable.

g^{n+1}_{c} that propagates in the positive z direction by

$$g^{n+1}_{\text{c}} = V^{n+1} + \hat{Z}_c I_z^{n+\frac{1}{2}}, \tag{37}$$

where V^{n+1} is the discrete potential difference between the inner probe and the outer shield of the coaxial cable, which is related to the discrete tangential electric fields at the bottom of the four Yee cells by

$$E^{n+1}_{x1}\Delta = -E^{n+1}_{x2}\Delta = E^{n+1}_{y1}\Delta = -E^{n+1}_{y2}\Delta = V^{n+1}. \tag{38}$$

Under the assumption that $\Delta x = \Delta y = \Delta z = \Delta$ inside Γ_{coax}, the discrete current $I_z^{n+\frac{1}{2}}$ represents a current flowing in the inner probe in the positive z direction and is given by

$$I_z^{n+\frac{1}{2}} = \frac{\pi\Delta}{4}(H_{y1}^{n+\frac{1}{2}} - H_{y2}^{n+\frac{1}{2}} + H_{x2}^{n+\frac{1}{2}} - H_{x1}^{n+\frac{1}{2}}). \tag{39}$$

Moreover, $\hat{Z}_c = Z_{\text{m}}\hat{\kappa}$ represents the intrinsic impedance of the discrete coaxial cable with $Z_{\text{m}} = \sqrt{\mu/\epsilon}$ and $\hat{\kappa} = 1/\pi$. Inside the coaxial cable, a signal h^{n+1}_{c} that propagates in the negative z direction is given by

$$h^{n+1}_{\text{c}} = V^{n+1} - \hat{Z}_c I_z^{n+\frac{1}{2}}. \tag{40}$$

Thus, we formulate a discrete version of the objective function (4) as

$$W^{\Delta}_{\text{out,coax}}(\boldsymbol{\sigma}) = \frac{1}{Z_m}\sum_{n=0}^{N}(V^{n+1} - \hat{Z}_{\text{c}} I_z^{n+\frac{1}{2}})^2\Delta t, \tag{41}$$

where $\boldsymbol{\sigma}$ indicates the conductivities located at each Yee edge inside Ω^{Δ}.

4.3. Discrete sensitivity analysis

In this section, we use the adjoint-field method to derive the derivatives of the discrete objective function (41) with respect to the conductivity vector $\boldsymbol{\sigma}$ that constitutes the design variables. When the conductivity vector $\boldsymbol{\sigma}$ is perturbed by $\delta\boldsymbol{\sigma}$, the corresponding first-order variation in the objective function is

$$\delta W^{\Delta}_{\text{out,coax}}(\boldsymbol{\sigma}) = \frac{2}{Z_m}\sum_{n=0}^{N}(V^{n+1} - \hat{Z}_{\text{c}} I_z^{n+\frac{1}{2}})(\delta V^{n+1} - \hat{Z}_{\text{c}}\delta I_z^{n+\frac{1}{2}})\Delta t, \tag{42}$$

where δV^{n+1} and $\delta I_z^{n+\frac{1}{2}}$ are the first-order variations of the discrete current and the discrete potential difference inside the coaxial cable, respectively. We depend on the FDTD discretization of Maxwell's equations (34) to find an explicit expression for the sensitivity of the objective function with respect to the design variables $\boldsymbol{\sigma}$.

We start by differentiating equations (34) with respect to $\boldsymbol{\sigma}$, which yields

$$\Big[D_t \delta B_{x,y,z} + \frac{\sigma^p_{y,z,x}}{\epsilon_0} S_t \delta B_{x,y,z} + \frac{1}{\mu_{x,y,z}}\big(D_{y,z,x}\delta E_{z,x,y} - D_{z,x,y}\delta E_{y,z,x}\big)\Big]\Big|^n = \mathbf{0}, \tag{43a}$$

$$\Big[D_t \delta H_{x,y,z} + \frac{\sigma^p_{z,x,y}}{\epsilon_0} S_t \delta H_{x,y,z} - D_t \delta B_{x,y,z} - \frac{\sigma^p_{x,y,z}}{\epsilon_0} S_t \delta B_{x,y,z}\Big]\Big|^n = \mathbf{0}, \tag{43b}$$

$$\Big[D_t \delta P_{x,y,z} + \frac{\sigma_{x,y,z}}{\epsilon_{x,y,z}} S_t \delta P_{x,y,z} + \frac{\delta\sigma_{x,y,z}}{\epsilon_{x,y,z}} S_t P_{x,y,z} - \frac{1}{\epsilon_{x,y,z}}\big(D_{y,z,x}\delta H_{z,x,y} - D_{z,x,y}\delta H_{y,z,x}\big)\Big]\Big|^{n+\frac{1}{2}} = \mathbf{0}, \tag{43c}$$

$$\Big[D_t \delta Q_{x,y,z} + \frac{\sigma^p_{z,x,y}}{\epsilon_0} S_t \delta Q_{x,y,z} - D_t \delta P_{x,y,z}\Big]\Big|^{n+\frac{1}{2}} = \mathbf{0}, \tag{43d}$$

$$\Big[D_t \delta E_{x,y,z} + \frac{\sigma^p_{y,z,x}}{\epsilon_0} S_t \delta E_{x,y,z} - D_t \delta Q_{x,y,z} - \frac{\sigma^p_{x,y,z}}{\epsilon_0} S_t \delta Q_{x,y,z}\Big]\Big|^{n+\frac{1}{2}} = \mathbf{0}. \tag{43e}$$

We introduce the grid functions $\boldsymbol{B}^*$, $\boldsymbol{H}^*$, $\boldsymbol{P}^*$, $\boldsymbol{Q}^*$, and $\boldsymbol{E}^*$, that are co-located with the grid points of $\boldsymbol{B}$, $\boldsymbol{H}$, $\boldsymbol{P}$, $\boldsymbol{Q}$, and $\boldsymbol{E}$, respectively. We require that these vectors satisfy the same boundary conditions as the forward fields, that is,

$$P_t^{*n} = Q_t^{*n} = E_t^{*n} = \mathbf{0} \qquad \text{on} \quad \partial\Omega^\Delta \setminus \partial\Gamma^\Delta_{\text{coax}}, \ \text{for } n = 0, \ldots, N. \tag{44}$$

We perform the scalar product of equations (43a), (43b), (43c), (43d), and (43e) with $\mu\boldsymbol{B}^*$, $\mu\boldsymbol{H}^*$, $\epsilon\boldsymbol{P}^*$, $\epsilon\boldsymbol{Q}^*$, and $\epsilon\boldsymbol{E}^*$, respectively. Then, we sum over the whole analysis domain $\Omega^\Delta_\infty = \Omega^\Delta \cup \Gamma^\Delta_{\text{coax}}$ through all the time steps, which yields

$$\begin{aligned}
\sum_{\Omega^\Delta_\infty}\sum_{n=0}^{N} & \mu_{x,y,z} B^*_{x,y,z}\Big[D_t \delta B_{x,y,z} + \frac{\sigma^p_{y,z,x}}{\epsilon_0} S_t \delta B_{x,y,z} + \frac{1}{\mu_{x,y,z}}\big(D_{y,z,x}\delta E_{z,x,y} - D_{z,x,y}\delta E_{y,z,x}\big)\Big]\Big|^n \\
&+ \mu_{x,y,z} H^*_{x,y,z}\Big[D_t \delta H_{x,y,z} + \frac{\sigma^p_{z,x,y}}{\epsilon_0} S_t \delta H_{x,y,z} - D_t \delta B_{x,y,z} - \frac{\sigma^p_{x,y,z}}{\epsilon_0} S_t \delta B_{x,y,z}\Big]\Big|^n \\
&+ \epsilon_{x,y,z} P^*_{x,y,z}\Big[D_t \delta P_{x,y,z} + \frac{\sigma_{x,y,z}}{\epsilon_{x,y,z}} S_t \delta P_{x,y,z} + \frac{\delta\sigma_{x,y,z}}{\epsilon_{x,y,z}} S_t P_{x,y,z} \\
&\qquad - \frac{1}{\epsilon_{x,y,z}}\big(D_{y,z,x}\delta H_{z,x,y} - D_{z,x,y}\delta H_{y,z,x}\big)\Big]\Big|^{n+\frac{1}{2}} \\
&+ \epsilon_{x,y,z} Q^*_{x,y,z}\Big[D_t \delta Q_{x,y,z} + \frac{\sigma^p_{z,x,y}}{\epsilon_0} S_t \delta Q_{x,y,z} - D_t \delta P_{x,y,z}\Big]\Big|^{n+\frac{1}{2}} \\
&+ \epsilon_{x,y,z} E^*_{x,y,z}\Big[D_t \delta E_{x,y,z} + \frac{\sigma^p_{y,z,x}}{\epsilon_0} S_t \delta E_{x,y,z} - D_t \delta Q_{x,y,z} - \frac{\sigma^p_{x,y,z}}{\epsilon_0} S_t \delta Q_{x,y,z}\Big]\Big|^{n+\frac{1}{2}} = 0.
\end{aligned} \tag{45}$$

Note that, in equation (45) the grid functions $\boldsymbol{B}^*$ and $\boldsymbol{H}^*$ are sampled at time n, while $\boldsymbol{P}^*$, $\boldsymbol{Q}^*$, and $\boldsymbol{E}^*$ are sampled at time $n + \frac{1}{2}$. We require the grid functions $\boldsymbol{B}^*$, $\boldsymbol{H}^*$, $\boldsymbol{P}^*$, $\boldsymbol{Q}^*$, and $\boldsymbol{E}^*$ to satisfy

$$B^{*\,N}_{x,y,z} = H^{*\,N}_{x,y,z} = P^{*\,N+\frac{1}{2}}_{x,y,z} = Q^{*\,N+\frac{1}{2}}_{x,y,z} = E^{*\,N+\frac{1}{2}}_{x,y,z} = \mathbf{0}. \tag{46}$$

The following summation by part rules for the time-domain finite-difference operators can be used,

$$\sum_{n=0}^{N} \nu^n D_t \delta u^n = -\sum_{n=0}^{N} \delta u^{n+1/2} D_t \nu^{n+1/2}, \tag{47a}$$

$$\sum_{n=0}^{N} \nu^n S_t \delta u^n = \sum_{n=0}^{N} \delta u^{n+1/2} S_t \nu^{n+1/2}, \tag{47b}$$

where the initial and steady state assumptions of equations (35) and (46) yield zero contributions from the terminal values. By using the boundary condition of equations (33) and (44), a similar summation by part rule can be used for the spatial finite-difference operators

$$\sum_{\Omega^\Delta_\infty} \nu^n D_{x,y,z} \delta u^n = -\sum_{\Gamma^\Delta_{\text{coax}}} \frac{\delta u^n \nu^n}{\Delta} - \sum_{\Omega^\Delta} \delta u^n D_{x,y,z} \nu^n, \tag{48}$$

where the first sum on the right evaluates to nonzero value only in $\Gamma^\Delta_{\text{coax}}$. Using the summation by part rules, equations (45) can be written as

$$\begin{aligned}
&\sum_{\Omega^\Delta}\sum_{n=0}^{N} \mu_{x,y,z}\delta B_{x,y,z}\Big[-D_t B^*_{x,y,z} + \frac{\sigma^p_{y,z,x}}{\epsilon_0} S_t B^*_{x,y,z} + D_t H^*_{x,y,z} - \frac{\sigma^p_{x,y,z}}{\epsilon_0} S_t H^*_{x,y,z}\Big]\Big|^{n+\frac{1}{2}} \\
&+\sum_{\Omega^\Delta}\sum_{n=0}^{N} \mu_{x,y,z}\delta H_{x,y,z}\Big[-D_t H^*_{x,y,z} + \frac{\sigma^p_{z,x,y}}{\epsilon_0} S_t H^*_{x,y,z} + \frac{1}{\mu_{x,y,z}} D_{z,x,y} P^*_{y,z,x} - \frac{1}{\mu_{x,y,z}} D_{y,z,x} P^*_{z,x,y}\Big]\Big|^{n+\frac{1}{2}} \\
&+\sum_{\Omega^\Delta}\sum_{n=0}^{N} \epsilon_{x,y,z}\delta P_{x,y,z}\Big[-D_t P^*_{x,y,z} + \frac{\sigma_{x,y,z}}{\epsilon_{x,y,z}} S_t P^*_{x,y,z} + D_t Q^*_{x,y,z}\Big]\Big|^{n+1} \\
&+\sum_{\Omega^\Delta}\sum_{n=0}^{N} \epsilon_{x,y,z}\delta Q_{x,y,z}\Big[-D_t Q^*_{x,y,z} + \frac{\sigma^p_{z,x,y}}{\epsilon_0} S_t Q^*_{x,y,z} + D_t E^*_{x,y,z} + \frac{\sigma^p_{x,y,z}}{\epsilon_0} S_t E^*_{x,y,z}\Big]\Big|^{n+1} \\
&+\sum_{\Omega^\Delta}\sum_{n=0}^{N} \epsilon_{x,y,z}\delta E_{x,y,z}\Big[-D_t E^*_{x,y,z} + \frac{\sigma^p_{y,z,x}}{\epsilon_0} S_t E^*_{x,y,z} - \frac{1}{\epsilon_{x,y,z}} D_{z,x,y} B^*_{y,z,x} + \frac{1}{\epsilon_{x,y,z}} D_{y,z,x} B^*_{z,x,y}\Big]\Big|^{n+1} \\
&+\sum_{\Omega^\Delta}\sum_{n=0}^{N} \Big(P_{x,y,z} S_t P^*_{x,y,z}\delta\sigma_{x,y,z}\Big)\Big|^{n+1} \\
&+\sum_{\Gamma^\Delta_{\text{coax}}}\sum_{n=0}^{N} \Big(\frac{\delta E_y B^*_x}{\Delta} - \frac{\delta E_x B^*_y}{\Delta}\Big)\Big|^{n+1} + \Big(\frac{\delta H_x P^*_y}{\Delta} - \frac{\delta H_y P^*_x}{\Delta}\Big)\Big|^{n+\frac{1}{2}} \\
&+\sum_{\Gamma^\Delta_{\text{coax}}}\sum_{n=0}^{N} \Big(\delta E_x D_y B^*_z - \delta E_y D_x B^*_z\Big)\Big|^{n+1} = 0.
\end{aligned} \tag{49}$$

By using equation (38), we can prove that

$$\sum_{\Gamma^\Delta_{\text{coax}}}\sum_{n=0}^{N} \Big(\delta E_x D_y B^*_z - \delta E_y D_x B^*_z\Big)\Big|^{n+1} = 0. \tag{50}$$

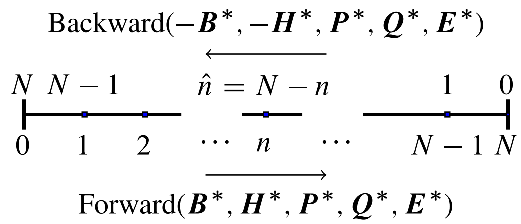

Figure 4. Changing the adjoint-problem from a terminal-value-problem to an initial-value-problem.

We now require that the expressions between brackets in equation (49) to vanish, that is

$$\Big[-D_t H^*_{x,y,z} + \frac{\sigma^p_{z,x,y}}{\epsilon_0} S_t H^*_{x,y,z} + \frac{1}{\mu_{x,y,z}}\big(D_{z,x,y} P^*_{y,z,x} - D_{y,z,x} P^*_{z,x,y}\big)\Big]\Big|^{n+\frac{1}{2}} = \mathbf{0}, \tag{51a}$$

$$\Big[-D_t B^*_{x,y,z} + \frac{\sigma^p_{y,z,x}}{\epsilon_0} S_t B^*_{x,y,z} + D_t H^*_{x,y,z} - \frac{\sigma^p_{x,y,z}}{\epsilon_0} S_t H^*_{x,y,z}\Big]\Big|^{n+\frac{1}{2}} = \mathbf{0}, \tag{51b}$$

$$\Big[-D_t E^*_{x,y,z} + \frac{\sigma^p_{y,z,x}}{\epsilon_0} S_t E^*_{x,y,z} - \frac{1}{\epsilon_{x,y,z}}\big(D_{z,x,y} B^*_{y,z,x} - D_{y,z,x} B^*_{z,x,y}\big)\Big]\Big|^{n+1} = \mathbf{0}, \tag{51c}$$

$$\Big[-D_t Q^*_{x,y,z} + \frac{\sigma^p_{z,x,y}}{\epsilon_0} S_t Q^*_{x,y,z} + D_t E^*_{x,y,z} + \frac{\sigma^p_{x,y,z}}{\epsilon_0} S_t E^*_{x,y,z}\Big]\Big|^{n+1} = \mathbf{0}, \tag{51d}$$

$$\Big[-D_t P^*_{x,y,z} + \frac{\sigma_{x,y,z}}{\epsilon_{x,y,z}} S_t P^*_{x,y,z} + D_t Q^*_{x,y,z}\Big]\Big|^{n+1} = \mathbf{0}. \tag{51e}$$

Then equation (49) reduces to

$$\begin{aligned}\sum_{\Omega^\Delta}\sum_{n=0}^{N}\Big(P_{x,y,z} S_t P^*_{x,y,z}\delta\sigma_{x,y,z}\Big)\Big|^{n+1} &= \\ -\frac{1}{\Delta}\sum_{\Gamma^\Delta_{\mathrm{coax}}}\sum_{n=0}^{N}\Big(\delta E_y B^*_x - \delta E_x B^*_y\Big)\Big|^{n+1} &+ \Big(\delta H_x P^*_y - \delta H_y P^*_x\Big)\Big|^{n+\frac{1}{2}}.\end{aligned} \tag{52}$$

Equations (51) are of a form similar to the standard FDTD update equations (34) but with the terminal condition assumed in equation (46),

$$B^{*\,N}_{x,y,z} = H^{*\,N}_{x,y,z} = P^{*\,N+\frac{1}{2}}_{x,y,z} = Q^{*\,N+\frac{1}{2}}_{x,y,z} = E^{*\,N+\frac{1}{2}}_{x,y,z} = \mathbf{0}.$$

This implies solving equations (51) backward in time which can be done by reversing the time axis and for consistency changing the sign of the grid functions corresponding to the magnetic fields (to preserve the Poynting vector direction), as shown in Figure 4. Then equations (51) can be written as

$$\left[D_t E^*_{x,y,z} + \frac{\sigma^p_{y,z,x}}{\epsilon_0} S_t E^*_{x,y,z} + \frac{1}{\epsilon_{x,y,z}}\left(D_{z,x,y} B^*_{y,z,x} - D_{y,z,x} B^*_{z,x,y}\right)\right]\Big|^{\hat{n}-1} = \mathbf{0}, \tag{53a}$$

$$\left[D_t Q^*_{x,y,z} + \frac{\sigma^p_{z,x,y}}{\epsilon_0} S_t Q^*_{x,y,z} - D_t E^*_{x,y,z} - \frac{\sigma^p_{x,y,z}}{\epsilon_0} S_t E^*_{x,y,z}\right]\Big|^{\hat{n}-1} = \mathbf{0}, \tag{53b}$$

$$\left[D_t P^*_{x,y,z} + \frac{\sigma_{x,y,z}}{\epsilon_{x,y,z}} S_t P^*_{x,y,z} - D_t Q^*_{x,y,z}\right]\Big|^{\hat{n}-1} = \mathbf{0}, \tag{53c}$$

$$\left[D_t H^*_{x,y,z} + \frac{\sigma^p_{z,x,y}}{\epsilon_0} S_t H^*_{x,y,z} - \frac{1}{\mu_{x,y,z}}\left(D_{z,x,y} P^*_{y,z,x} - D_{y,z,x} P^*_{z,x,y}\right)\right]\Big|^{\hat{n}-\frac{1}{2}} = \mathbf{0}, \tag{53d}$$

$$\left[D_t B^*_{x,y,z} + \frac{\sigma^p_{y,z,x}}{\epsilon_0} S_t B^*_{x,y,z} - D_t H^*_{x,y,z} - \frac{\sigma^p_{x,y,z}}{\epsilon_0} S_t H^*_{x,y,z}\right]\Big|^{\hat{n}-\frac{1}{2}} = \mathbf{0}, \tag{53e}$$

with the initial conditions

$$B^{*\,0}_{x,y,z} = H^{*\,0}_{x,y,z} = P^{*\,-\frac{1}{2}}_{x,y,z} = Q^{*\,-\frac{1}{2}}_{x,y,z} = E^{*\,-\frac{1}{2}}_{x,y,z} = \mathbf{0}. \tag{54}$$

Equations (53) are the FDTD discretization of the system

$$\left(\frac{\partial}{\partial t} + \sigma^{p_3}\right) \boldsymbol{H}^* + \frac{1}{\mu}\nabla \times \boldsymbol{P}^* = \mathbf{0}, \tag{55a}$$

$$\left(\frac{\partial}{\partial t} + \sigma^{p_2}\right) \boldsymbol{B}^* - \left(\frac{\partial}{\partial t} + \sigma^{p_1}\right) \boldsymbol{H}^* = \mathbf{0}, \tag{55b}$$

$$\left(\frac{\partial}{\partial t} + \sigma^{p_2}\right) \boldsymbol{E}^* - \frac{1}{\epsilon}\nabla \times \boldsymbol{B}^* = \mathbf{0}, \tag{55c}$$

$$\left(\frac{\partial}{\partial t} + \sigma^{p_3}\right) \boldsymbol{Q}^* - (\frac{\partial}{\partial t} + \sigma^{p_1})\boldsymbol{E}^* = \mathbf{0}, \tag{55d}$$

$$\left(\frac{\partial}{\partial t} + \sigma\right) \boldsymbol{P}^* - \frac{\partial}{\partial t}\boldsymbol{Q}^* = \mathbf{0}. \tag{55e}$$

Equations (55) can be seen as a version of Maxwell's equations in the primal field vectors $\boldsymbol{P}^*$ and $\boldsymbol{B}^*$, and the auxiliary field vectors $\boldsymbol{H}^*$, $\boldsymbol{E}^*$, and $\boldsymbol{Q}^*$ are used for the implementation of the UPML. However, the auxiliary equations that implement the UPML in equations (55) are arranged in a different order compared to the forward equations (27). This means that, inside the PML-free region (i.e. when $\sigma^p_i = 0$) the discretization of the adjoint equations (55) and the forward equations (34) are the same, and the same FDTD code can be used to update the primal fields. We will discuss this issue later in the next section.

Similar to the forward system, we set the transverse field $\boldsymbol{P}^*_t$ at the bottom of the discrete coaxial feed to satisfy

$$P^{*\,n+\frac{1}{2}}_{x1}\Delta = -P^{*\,n+\frac{1}{2}}_{x2}\Delta = P^{*\,n+\frac{1}{2}}_{y1}\Delta = -P^{*\,n+\frac{1}{2}}_{y2}\Delta = V^{*\,n+\frac{1}{2}} \quad \text{on} \quad \Gamma^{\Delta}_{\text{coax}}, \tag{56}$$

where $V^{*\,n+\frac{1}{2}}$ indicates a discrete adjoint potential difference between the inner and the outer conductors of the coaxial cable with P^*_i has the same spatial distribution as E_i in Figure 3. By using equations (38), (39), and (56), equation (52) can be written as

$$\begin{aligned}\sum_{\Omega^\Delta}\sum_{n=0}^{N}\left(P_{x,y,z} S_t P^*_{x,y,z}\delta\sigma_{x,y,z}\right)\Big|^{n+1} &= \\ -\frac{1}{\Delta}\sum_{n=0}^{N}\left(\frac{\delta V}{\Delta}(B^*_{x1} - B^*_{x2} - B^*_{y1} + B^*_{y2})\right)\Big|^{n+1} &+ \frac{4}{\pi\Delta^2}V^{*\,n+\frac{1}{2}}\delta I_z^{n+\frac{1}{2}},\end{aligned} \tag{57}$$

where B^*_i has the same spatial distribution as H_i in Figure 3. We define an adjoint current $I_z^{*\,n+1}$ as

$$I_z^{*\,n+1} = \frac{\pi\Delta}{4}(B^{*\,n+1}_{y1} - B^{*\,n+1}_{y2} + B^{*\,n+1}_{x2} - B^{*\,n+1}_{x1}). \tag{58}$$

By differentiating equation (37), we obtain

$$0 = \delta V^{n+1} + \hat{Z}_c \delta I_z^{n+\frac{1}{2}}. \tag{59}$$

By using equations (59) and (58), equation (57) can be written as

$$\sum_{\Omega^\Delta} \sum_{n=0}^{N} \Big(P_{x,y,z} S_t P^*_{x,y,z} \delta\sigma_{x,y,z} \Big)\Big|^{n+1} = -\frac{4}{\pi \hat{Z}_c \Delta^3} \sum_{n=0}^{N} \delta V^{n+1} \Big(V^{*\,n+\frac{1}{2}} - \hat{Z}_c I_z^{*\,n+1} \Big). \tag{60}$$

Moreover, by expression (59) we can write

$$\delta V^{n+1} = \frac{1}{2}(\delta V^{n+1} - \hat{Z}_c \delta I_z^{n+\frac{1}{2}}).$$

Thus, if we select

$$\begin{aligned} (V^{*\,n+\frac{1}{2}} - \hat{Z}_c I_z^{*\,n+1}) &= (V^{n+1} - \hat{Z}_c I_z^{n+\frac{1}{2}}) \qquad \text{for} \quad n = 0, \dots, N \\ &= (V^{*\,\hat{n}-\frac{1}{2}} + \hat{Z}_c I_z^{*\,\hat{n}-1}), \end{aligned} \tag{61}$$

then equation (60) can be written as

$$\begin{aligned} &-\Delta^3 \sum_{\Omega^\Delta} \sum_{n=0}^{N} \Big(P_{x,y,z} S_t P^*_{x,y,z} \delta\sigma_{x,y,z} \Delta t \Big)\Big|^{n+1} = \\ &\qquad \frac{2}{Z_m} \sum_{n=0}^{N} (\delta V^{n+1} - \hat{Z}_c \delta I^{n+\frac{1}{2}})(V^{n+1} - \hat{Z}_c I_z^{n+\frac{1}{2}}) \Delta t. \end{aligned} \tag{62}$$

The right hand side of equation (62) represents the directional derivative of the objective function $W^\Delta_{\text{out,coax}}(\boldsymbol{\sigma})$ (given in equation (42)) when the conductivity is perturbed by $\delta\sigma$. The derivatives of the objective function with respect to the pointwise conductivities σ_i located at the i^{th} Yee edge, can be written as

$$\frac{\partial W^\Delta_{\text{out,coax}}}{\partial \sigma_i} = -\Delta^3 \sum_{\hat{n}=1}^{N} P_i^{N-\hat{n}} \frac{P_i^{*\,\hat{n}-\frac{1}{2}} + P_i^{*\,\hat{n}+\frac{1}{2}}}{2} \Delta t. \tag{63}$$

4.4. Summarizing the sensitivity calculations

We summarize the derivatives calculations based on the FDTD method in three steps. First, we use the FDTD method to solve the forward system over the analysis domain Ω^Δ_∞, where we store the outgoing signal $V^{n+1} - \hat{Z}_c I_z^{n+1/2}$ (used also to evaluate the objective function) and the electric field $\boldsymbol{E}$ ($\boldsymbol{E} = \boldsymbol{P}$ in the PML-free region) in the design domain for $n = 0, 1, \ldots, N$. The forward system is summarized as,

$$\left(\frac{\partial}{\partial t} + \sigma^{p_2}\right) \boldsymbol{B} + \frac{1}{\mu}\nabla \times \boldsymbol{E} = \boldsymbol{0}, \tag{64a}$$

$$\left(\frac{\partial}{\partial t} + \sigma^{p_3}\right) \boldsymbol{H} - (\frac{\partial}{\partial t} + \sigma^{p_1})\boldsymbol{B} = \boldsymbol{0}, \tag{64b}$$

$$\left(\frac{\partial}{\partial t} + \frac{\sigma}{\epsilon}\right) \boldsymbol{P} - \frac{1}{\epsilon}\nabla \times \boldsymbol{H} = \boldsymbol{0}, \tag{64c}$$

$$\left(\frac{\partial}{\partial t} + \sigma^{p_3}\right) \boldsymbol{Q} - \frac{\partial}{\partial t}\boldsymbol{P} = \boldsymbol{0}, \tag{64d}$$

$$\left(\frac{\partial}{\partial t} + \sigma^{p_2}\right) \boldsymbol{E} - \left(\frac{\partial}{\partial t} + \sigma^{p_1}\right) \boldsymbol{Q} = \boldsymbol{0}, \tag{64e}$$

$$B_{x,y,z}^{-\frac{1}{2}} = H_{x,y,z}^{-\frac{1}{2}} = P_{x,y,z}^{0} = Q_{x,y,z}^{0} = E_{x,y,z}^{0} = \boldsymbol{0} \qquad \text{in } \Omega_\infty^\Delta, \tag{64f}$$

$$P_t^n = Q_t^n = E_t^n = \boldsymbol{0} \qquad \text{on } \partial\Omega^\Delta \setminus \partial\Gamma_{\text{coax}}^\Delta, n = 0, \ldots, N, \tag{64g}$$

$$E_{x1}^{n+1}\Delta = -E_{x2}^{n+1}\Delta = E_{y1}^{n+1}\Delta = -E_{y2}^{n+1}\Delta = V^{n+1} \qquad \text{on } \partial\Gamma_{\text{coax}}^\Delta, n = 0, \ldots, N, \tag{64h}$$

$$I_z^{n+\frac{1}{2}} = \frac{\pi\Delta}{4}(H_{y1}^{n+\frac{1}{2}} - H_{y2}^{n+\frac{1}{2}} + H_{x2}^{n+\frac{1}{2}} - H_{x1}^{n+\frac{1}{2}}) \qquad \text{in } \Gamma_{\text{coax}}^\Delta, n = 0, \ldots, N, \tag{64i}$$

$$V^{n+1} + \hat{Z}_c I_z^{n+\frac{1}{2}} = g_c^{n+1} \qquad \text{for} \quad n = 0, \ldots, N, \tag{64j}$$

$$W_{\text{out,coax}}^\Delta(\boldsymbol{\sigma}) = \frac{1}{Z_m}\sum_{n=0}^{N}(V^{n+1} - \hat{Z}_c I_z^{n+\frac{1}{2}})^2 \Delta t. \tag{64k}$$

Second, we solve the FDTD discretization of the following system over the analysis domain Ω_∞^Δ, where we store the adjoint-field $\boldsymbol{P}^*$ at the design domain for $\hat{n} = 0, 1, \ldots, N$,

$$\left(\frac{\partial}{\partial t} + \sigma^{p_3}\right) \boldsymbol{H}^* + \frac{1}{\mu}\nabla \times \boldsymbol{P}^* = \boldsymbol{0}, \tag{65a}$$

$$\left(\frac{\partial}{\partial t} + \sigma^{p_2}\right) \boldsymbol{B}^* - \left(\frac{\partial}{\partial t} + \sigma^{p_1}\right) \boldsymbol{H}^* = \boldsymbol{0}, \tag{65b}$$

$$\left(\frac{\partial}{\partial t} + \sigma^{p_2}\right) \boldsymbol{E}^* - \frac{1}{\epsilon}\nabla \times \boldsymbol{B}^* = \boldsymbol{0}, \tag{65c}$$

$$\left(\frac{\partial}{\partial t} + \sigma^{p_3}\right) \boldsymbol{Q}^* - (\frac{\partial}{\partial t} + \sigma^{p_1})\boldsymbol{E}^* = \boldsymbol{0}, \tag{65d}$$

$$\left(\frac{\partial}{\partial t} + \sigma\right) \boldsymbol{P}^* - \frac{\partial}{\partial t}\boldsymbol{Q}^* = \boldsymbol{0}, \tag{65e}$$

$$B_{x,y,z}^{*\,0} = H_{x,y,z}^{*\,0} = P_{x,y,z}^{*\,-\frac{1}{2}} = Q_{x,y,z}^{*\,-\frac{1}{2}} = E_{x,y,z}^{*\,-\frac{1}{2}} = \boldsymbol{0} \qquad \text{in } \Omega_\infty^\Delta, \tag{65f}$$

$$P_t^{*\,\hat{n}} = Q_t^{*\,\hat{n}} = E_t^{*\,\hat{n}} = \boldsymbol{0} \qquad \text{on } \partial\Omega^\Delta \setminus \partial\Gamma_{\text{coax}}^\Delta, \hat{n} = 0, \ldots, N, \tag{65g}$$

$$P_{x1}^{*\,\hat{n}+\frac{1}{2}}\Delta = -P_{x2}^{*\,\hat{n}+\frac{1}{2}}\Delta = P_{y1}^{*\,\hat{n}+\frac{1}{2}}\Delta = -P_{y2}^{*\,\hat{n}+\frac{1}{2}}\Delta = V^{*\,\hat{n}+\frac{1}{2}} \qquad \text{on } \partial\Gamma_{\text{coax}}^\Delta, \hat{n} = 0, \ldots, N, \tag{65h}$$

$$I_z^{*\,\hat{n}+1} = \frac{\pi\Delta}{4}(B_{y1}^{*\,\hat{n}+1} - B_{y2}^{*\,\hat{n}+1} + B_{x2}^{*\,\hat{n}+1} - B_{x1}^{*\,\hat{n}+1}) \qquad \text{in } \Gamma_{\text{coax}}^\Delta, \hat{n} = 0, \ldots, N, \tag{65i}$$

$$V^{*\,\hat{n}-\frac{1}{2}} + \hat{Z}_c I_z^{*\,\hat{n}-1} = (V^{N-\hat{n}+1} - \hat{Z}_c I^{N-\hat{n}+\frac{1}{2}}) \qquad \text{for} \quad \hat{n} = 1, \ldots, N. \tag{65j}$$

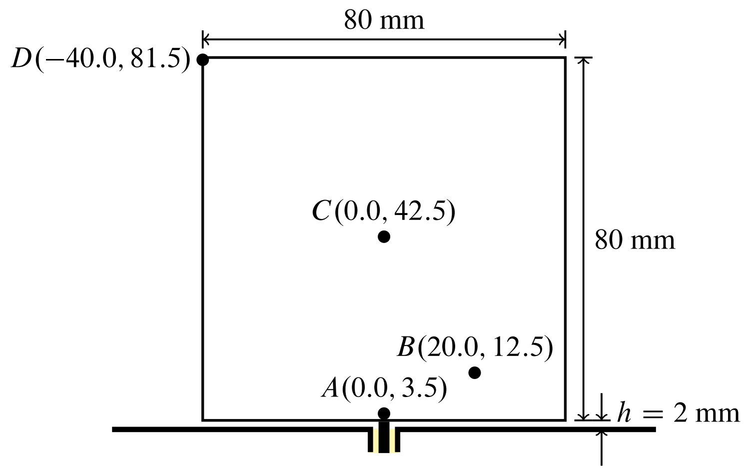

Figure 5. A 80×80 mm^2 design domain located 2 mm above the ground plane and connected to a 50 Ω coaxial cable at the center.

Third, we compute the gradient vector using the following expression,

$$\frac{\partial W^{\Delta}_{\text{out,coax}}}{\partial \sigma_i} = -\Delta^3 \sum_{\hat{n}=1}^{N} E_i^{N-\hat{n}} \frac{P_i^{*\,\hat{n}-\frac{1}{2}} + P_i^{*\,\hat{n}+\frac{1}{2}}}{2} \, \Delta t. \tag{66}$$

As we pointed out earlier, the adjoint system and the forward system are equivalent inside the PML-free region. However, the two systems of equations are different in how the UPML is implemented by the auxiliary field vectors. To obtain exact gradient by using expression (66), up to roundoff, the FDTD discretization of the two system require two different FDTD codes that have two different UPML implementation to simulate the open space radiation condition. To avoid using two different FDTD codes, we use the UPML implementation of the forward system with the adjoint system, as well. In the next section, we give some numerical experiments that compare the accuracy of the calculated derivatives by using (66), with the UPML modification, compared with the derivatives calculated by using the finite difference approximations.

5. NUMERICAL EXAMPLE

In this section, we compute the derivatives of the outgoing signal through the coaxial cable with respect to the conductivity distribution in a specific domain. We compare the values of the calculated derivatives using expression (66) with the values obtained by finite difference expression (2). Further, we use the Richardson extrapolation technique [10] to improve the accuracy of derivatives computed with finite differences.

We consider a planar domain Ω located in the yz plane with dimensions 80×80 mm^2, as shown in Figure 5. The domain Ω is located 2 mm above an infinite simulated ground plane that resides in the xy plane. A 50 Ω coaxial cable is located at the origin $(0, 0, 0)$ and its inner probe is connected to the center of the bottom side of Ω. We compute the pointwise derivative of the outgoing signal inside the coaxial cable with respect to conductivities located at four points inside the domain Ω. The four points are located at $A = (0, 0, 3.5)$, $B = (0, 20, 12.5)$, $C = (0, 0, 42.5)$, and $D = (0, -40, 81.5)$ (dimensions are in mm). Here, we excite the analysis domain through the coaxial cable with a signal that covers the frequency band from 1 to 10 GHz.

The whole domain Ω is assumed to have the same conductivity value σ when the derivatives are computed. The derivatives of the objective function with respect to the conductivity at the four points A, B, C, and D are summarized in Table 1 for different conductivity values. We select a set of seven conductivity values, $\sigma = 10^n$ (S/m), $n = -2, -1, \ldots, 4$, which fall between the conductivity of a good dielectric and the conductivity of a good conductor at the frequency band of interest [1, 17]. In the table, we include the derivatives obtained by using the adjoint-field method together with the derivatives computed with the extrapolated finite differences. As can be noted from Table 1, the computed derivatives depend on the location of the point as well as on the value of the conductivity. The sensitivity of the objective function is much larger for points that are closer to the coaxial feed (for example at point A), which is expected for this kind of problems. We obtain up to 7 digits precision matching between the pointwise derivatives computed using the two methods. The adjoint sensitivity analysis introduced here is used in different antenna design problems [11, 18, 19].

Table 1. Derivatives of the outgoing signal in the coaxial cable with respect to the conductivity located at points A, B, C, and D (Figure 5). The derivatives are computed by the adjoint-field method and by the extrapolated finite differences for different conductivity values.

$\sigma(S/m)$	$\partial W^{\Delta}_{\text{out,coax}}/\partial\sigma$	Point A	Point B	Point C	Point D
10^{-2}	Adjoint method	-2.0068825e-01	4.5878325e-06	-7.1022153e-08	4.4145749e-09
	Finite difference	-2.0068841e-01	4.5872729e-06	-7.1057002e-08	4.4674379e-09
10^{-1}	Adjoint method	-2.0079936e-01	4.6801011e-06	-5.1879855e-08	3.4840560e-09
	Finite difference	-2.0079954e-01	4.6800590e-06	-5.1824870e-08	3.4815457e-08
10^{0}	Adjoint method	-1.8487441e-01	1.1236669e-06	4.1804294e-08	5.9458220e-11
	Finite difference	-1.8487455e-01	1.1236825e-06	4.1803370e-08	5.6729732e-11
10^{1}	Adjoint method	-1.3651086e-02	2.0281435e-07	2.7351293e-07	-8.9707997e-09
	Finite difference	-1.3651102e-02	2.0281842e-07	2.7351479e-07	-8.9702515e-09
10^{2}	Adjoint method	1.4386164e-04	-9.4098646e-09	-1.2208819e-08	3.1829860e-08
	Finite difference	1.4386133e-04	-9.4098773e-09	-1.2208720e-08	3.1829820e-08
10^{3}	Adjoint method	1.1269535e-06	-1.6704827e-09	-3.9989626e-10	2.2961594e-09
	Finite difference	1.1269527e-06	-1.6704847e-09	-3.9988207e-10	2.2961561e-09
10^{4}	Adjoint method	1.2216764e-08	-2.0837589e-11	-4.4090082e-12	2.9548610e-11
	Finite difference	1.2216762e-08	-2.0838893e-11	-4.4074327e-12	2.9546927e-11
Best # of digits match		7	6	5	6
Worst # of digits match		5	4	3	1

Summary

We introduced a problem formulation to calculate the sensitivity of the outgoing signals in coaxial cables with respect to conductivity distribution in a given domain. We used the adjoint-field method to present the derivative expressions. We derived two expressions based on the 3D time-domain Maxwell's equations; one in the continuous case and one in the discrete case based on the FDTD discretization of Maxwell's equations. We gave a numerical example to validate the derivatives calculated by using the derived expression against derivatives computed with finite differences. By using the adjoint-field method, the derivatives can be calculated for a large number of design variables in an accurate and efficient way. For any number of design variables the derivatives computation require only two solutions to Maxwell's equations by the FDTD method. The derived expression can be used to design electromagnetic devices that are generally connected to coaxial cables.

REFERENCES

1. Balanis, C. A., *Advanced Engineering Electromagnetics*. John Wiley & Sons, 1989.
2. Nikolova, N., Tam, H., and Bakr, M., "Sensitivity analysis with the FDTD method on structured grids," *IEEE Trans. Microw. Theory Tech.*, vol. 52, pp. 1207–1216, Apr. 2004.
3. Chung, Y.-S., Cheon, C., Park, I.-H., and Hahn, S.-Y., "Optimal design method for microwave device using time domain method and design sensitivity analysis. II. FDTD case," *IEEE Trans. Magn.*, vol. 37, pp. 3255–3259, Sep. 2001.
4. Kiziltas, G., Psychoudakis, D., Volakis, J., and Kikuchi, N., "Topology design optimization of dielectric substrates for bandwidth improvement of a patch antenna," *IEEE Trans. Antennas Propag.*, vol. 51, pp. 2732–2743, Oct. 2003.

5. Dyck, D. and Lowther, D., "Automated design of magnetic devices by optimizing material distribution," *IEEE Trans. Magn.*, vol. 32, pp. 1188–1193, May 1996.
6. Abenius, E., *Direct and Inverse Methods for Waveguides and Scattering Problems in the Time Domain*. PhD thesis, Uppsala University, 2005.
7. Nomura, T., Sato, K., Taguchi, K., Kashiwa, T., and Nishiwaki, S., "Structural topology optimization for the design of broadband dielectric resonator antennas using the finite difference time domain technique," *Int. J. Num. Meth. Eng.*, vol. 71, pp. 1261–1296, 2007.
8. Dyck, D., Lowther, D., and Freeman, E., "A method of computing the sensitivity of electromagnetic quantities to changes in materials and sources," *IEEE Trans. Magn.*, vol. 30, pp. 3415–3418, Sep. 1994.
9. Swillam, M., Bakr, M., Nikolova, N., and Li, X., "Adjoint Sensitivity Analysis of Dielectric Discontinuities Using FDTD," *Electromagnetics*, vol. 27, pp. 123–140, 2007.
10. Gautschi, W., *Numerical analysis: an introduction*. Cambridge, MA, USA: Birkhauser Boston Inc., 1997.
11. Hassan, E., Wadbro, E., and Berggren, M., "Topology optimization of metallic antennas," *IEEE Trans. Antennas Propag.*, vol. 62, pp. 2488–2500, May 2014.
12. Sun, W. and Yuan, Y., *Optimization theory and methods: nonlinear programming*. Springer-Verlag New York Inc., 2006.
13. Yee, K., "Numerical solution of initial boundary value problems involving maxwell's equations in isotropic media," *IEEE Trans. Antennas Propag.*, vol. 14, pp. 302–307, May 1966.
14. Taflove, A. and Hagness, S., *Computational Electrodynamics: The Finite-Difference Time-Domain Method*. Artech House, third ed., 2005.
15. Inan, U. S. and Marshall, R. A., *Numerical Electromagnetics: The FDTD Method*. Cambridge University Press, 2011.
16. Gedney, S., "An anisotropic perfectly matched layer-absorbing medium for the truncation of FDTD lattices," *IEEE Trans. Antennas Propag.*, vol. 44, pp. 1630–1639, Dec. 1996.
17. Jordan, E. C. and Balmain, K. G., *Electromagnetic waves and radiating systems*. Englewood Cliffs, N.J. : Prentice-Hall, 2nd ed ed., 1968.
18. Hassan, E., Wadbro, E., and Berggren, M., "Topology optimization of UWB monopole antennas," in *7th European Conference on Antennas and Propagation (EuCAP 2013)*, (Gothenburg, Sweden), Apr. 2013.
19. Hassan, E., Wadbro, E., and Berggren, M., "Patch and ground plane design of microstrip antennas by material distribution topology optimization," *Progress In Electromagnetics Research B*, vol. 59, pp. 89–102, 2014.